

# Simulation of the hybrid Tunka Advanced International Gamma-ray and Cosmic ray Astrophysics (TAIGA)

M Kunnas<sup>5</sup>, I Astapov<sup>8</sup>, N Barbashina<sup>8</sup>, S Beregnev<sup>11</sup>, A Bogdanov<sup>4</sup>,  
D Bogorodskii<sup>1</sup>, V Boreyko<sup>9</sup>, M Brückner<sup>2</sup>, N Budnev<sup>1</sup>, A  
Chiavassa<sup>6</sup>, O Chvalaev<sup>1</sup>, A Dyachok<sup>1</sup>, S Epimakhov<sup>5</sup>, T Eremin<sup>11</sup>, A  
Gafarov<sup>1</sup>, N Gorbunov<sup>9</sup>, V Grebenyuk<sup>9</sup>, O Gress<sup>1</sup>, T Gress<sup>1</sup>, A  
Grinyuk<sup>9</sup>, O Grishin<sup>1</sup>, D Horns<sup>5</sup>, A Ivanova<sup>1</sup>, N Karpov<sup>11</sup>, N  
Kalmykov<sup>11</sup>, Y Kazarina<sup>1</sup>, V Kindin<sup>4</sup>, N Kirichkov<sup>1</sup>, S Kiryuhin<sup>1</sup>, R  
Kokoulin<sup>4</sup>, K Kompaniets<sup>4</sup>, E Konstantinov<sup>1</sup>, A Korobchenko<sup>1</sup>, E  
Korosteleva<sup>11</sup>, V Kozhin<sup>11</sup>, L Kuzmichev<sup>11</sup>, V Lenok<sup>1</sup>, B  
Lubsandorzhev<sup>10</sup>, N Lubsandorzhev<sup>11</sup>, R Mirgazov<sup>1</sup>, R Mirzoyan<sup>7,1</sup>,  
R Monkhoev<sup>1</sup>, R Nachtigall<sup>5</sup>, A Pakhorukov<sup>1</sup>, M Panasyuk<sup>11</sup>, L  
Pankov<sup>1</sup>, A Perevalov<sup>1</sup>, A Petrukhin<sup>4</sup>, V Platonov<sup>1</sup>, V Poleschuk<sup>1</sup>, M  
Popescu<sup>12</sup>, E Popova<sup>11</sup>, A Porelli<sup>3</sup>, S Porokhovoy<sup>9</sup>, V Prosin<sup>11</sup>, V  
Ptuskin<sup>8</sup>, V Romanov<sup>9</sup>, G I Rubtsov<sup>10</sup>, Müger<sup>23</sup>, E Rybov<sup>1</sup>, V  
Samoliga<sup>1</sup>, P Satunin<sup>10</sup>, A Saunkin<sup>1</sup>, V Savinov<sup>1</sup>, Yu Semeney<sup>1</sup>, B  
Shaibonov(junior)<sup>10</sup>, A Silaev<sup>11</sup>, A Silaev (junior)<sup>11</sup>, A Skurikhin<sup>11</sup>, M  
Slunicka<sup>9</sup>, C Spiering<sup>3</sup>, L Sveshnikova<sup>11</sup>, V Tabolenko<sup>1</sup>, A  
Tkachenko<sup>9</sup>, L Tkachev<sup>9</sup>, M Tluczykont<sup>5</sup>, A Veslopopov<sup>1</sup>, E  
Veslopopova<sup>1</sup>, D Voronov<sup>1</sup>, R Wischnewski<sup>3</sup>, I Yashin<sup>4</sup>, K Yurin<sup>4</sup>, A  
Zagorodnikov<sup>1</sup>, V Zirakashvili<sup>8</sup>, V Zurbanov<sup>1</sup>,

<sup>1</sup>Institute of Applied Physics, Irkutsk State University, Irkutsk, Russia

<sup>2</sup>Institute for Computer Science, Humboldt-University Berlin, Rudower Chaussee 25, 12489  
Berlin, Germany

<sup>3</sup>DESY, Platanenallee 6, 15738 Zeuthen, Germany

<sup>4</sup>MEPhI (Moscow Engineering Physics Institute), National Research Nuclear University,  
Moscow, Russia

<sup>5</sup>Institut für Experimentalphysik, Luruper Chaussee 149, 22761 Hamburg, Germany

<sup>6</sup>Dipartimento di Fisica Generale Universiteta di Torino and INFN, Torino, Italy

<sup>7</sup>Werner Heisenberg Institut, Föhringer Ring 6, 80805, München, Germany

<sup>8</sup>IZMIRAN, Troitsk, Moscow Region, Russia

<sup>9</sup>Joint Institute for Nuclear Research, Joliot-Curie 6, 141980 Dubna, Moscow region, Russia

<sup>10</sup>Institute for Nuclear Research of the Russian Academy of Sciences 60th October  
Anniversary st., 7a, 117312, Moscow, Russia

<sup>11</sup>Skobel'syn institute for Nuclear Physics, Lomonosov Moscow State University, 1 Leninskie  
gory, 119991 Moscow, Russia

<sup>12</sup>Institute of Space Science, Bucharest, Romania

E-mail: maike.kunnas@physik.uni-hamburg.de



**Abstract.**

Up to several 10s of TeV, Imaging Air Cherenkov Telescopes (IACTs) have proven to be the instruments of choice for GeV/TeV gamma-ray astronomy due to their good reconstruction quality and gamma-hadron separation power. However, sensitive observations at and above 100 TeV require very large effective areas (10 km<sup>2</sup> and more), which is difficult and expensive to achieve.

The alternative to IACTs are shower front sampling arrays (non-imaging technique or timing-arrays) with a large area and a wide field of view. Such experiments provide good core position, energy and angular resolution, but only poor gamma-hadron separation. Combining both experimental approaches, using the strengths of both techniques, could optimize the sensitivity to the highest energies.

The TAIGA project plans to combine the non-imaging HiSCORE [8] array with small (~10m<sup>2</sup>) imaging telescopes. This paper covers simulation results of this hybrid approach.

**1. A hybrid system**

A pure IACT system uses two or more telescopes with (most often tessellated) mirrors and multi-channel cameras to take images of extensive air showers (EAS). These images give a good estimation of the nature of the primary particle, but incident angle and core position can only be precisely reconstructed if more than one image of a shower is taken. This sets an upper limit to the spacing of the telescopes of about 300 m since the telescopes need to be inside the Cherenkov light cone of the shower. But for high energy measurements, one requires huge effective areas due to the low flux, which means a huge area needs to be covered with detectors, and that is too expensive to do with telescopes.

On the other hand, shower front sampling array stations are (comparatively) cheap and give a good reconstruction of core position and incident angle, but the gamma hadron separation power is only weak at the threshold energies (~10 TeV)[2].

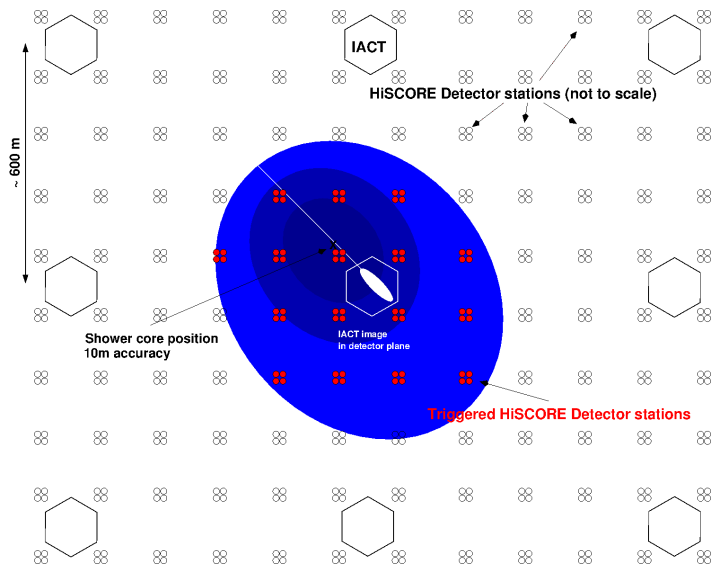


**Figure 1.** Principle for the combination of IACT and shower front sampling array observation.

To cover a large area with detectors, we want to increase the spacing of our telescopes to about 600 m. This way, the showers are seen by only one telescope at a time, but the reconstruction of these monoscopic images can benefit from the HiSCORE timing array, combining both techniques' strengths and canceling out their weaknesses: Taking the core position and incident angle from the shower front sampling array removes the IACT's need for stereoscopy, thus

enables an increase of telescope spacing without loss of gamma hadron separation power and therefore makes it possible to cover large areas with fewer telescopes (also see Tluczykont et al, these proceedings).

TAIGA itself will be a combination of small IACT telescopes (in development), the HiSCORE array (Hundred \* i Square-km Cosmic Origin Explorer, shower front sampling array, currently in deployment)[10] and the Tunka-Grande scintillation array (photon-electron and muon detection, planned) at Tunka valley, Russia (51° 48' 35" N, 103° 04' 02" E, 675 m a.s.l.). The muon detectors are envisaged for gamma-hadron separation at energies beyond 100 TeV. In the future, a radio extension is planned succeeding Tunka-Rex [12]. This paper will focus on the combination of the shower front sampling array and the IACTs.

The intended telescope parameters are:

- 4.3 m tessellated mirror dish, Davies-Cotton design
- Mirror segment diameter 60 cm, 34 segments
- 4.75 m focal length
- 8° telescope Field of View (FoV)
- 397 camera pixels with about 0.38° FoV each
- 600 m spacing

The HiSCORE sampling array consists of photomultiplier tubes (PMTs) looking directly into the sky through Winston Cones with 4 PMTs per station and about 120 m spacing between stations. Since 10/2013 a 9 station engineering array is running and a 28 station array is installed since 2014, allowing to start observation of the most bright gamma-sources. In the future, a large array of the order of 10 km<sup>2</sup> is envisaged.

## 2. Simulation

To evaluate the telescope design and gamma hadron separation power of the system, a Monte-Carlo (MC) simulation of the joint operation of the Tunka-HiSCORE wide-angle array and a Cherenkov telescope with image analysis is carried out. The efficiency of hadron background suppression (Q-factor) under gamma-quanta events separation is evaluated. This simulation is done in two steps:

1. Raw MC air shower data are generated with the CORSIKA code [3] including the package for EAS Cherenkov light data (IACT option, hadronic interaction models QGSJET [4] and Gheisha [5]). Here the nature of the primary and its properties (energy range, zenith angle, number of showers) are chosen by the user as well as the detector layout, i.e. the telescope/station positions.

2a. From the CORSIKA output the IACT response simulation with `sim_telarray` [6] is run. `sim_telarray` executes a raytracing routine with an automatic reconstruction of the MC images (see fig. 2, though manual reconstruction is possible) and includes all the important details of the telescope design, for example:

- Mirror dish configuration
- Mirror details
- Camera configuration
- Camera details (PMT response, funnels etc.)
- Electronic response
- Mast and camera shadowing

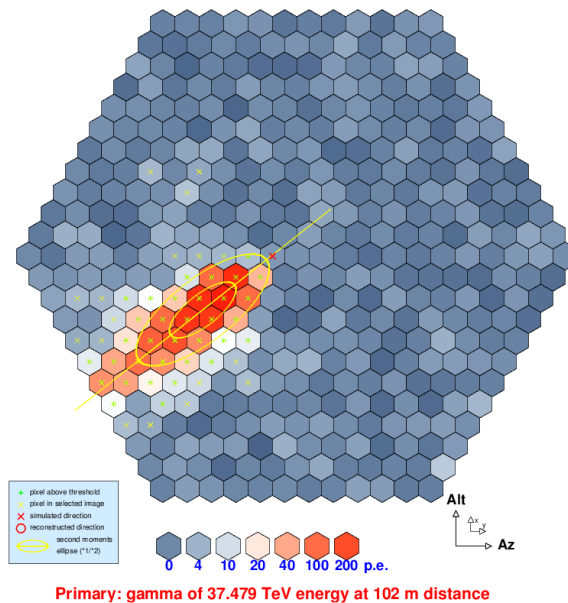


**Figure 2.** Example for a sim\_telarray-generated EAS image of a 37.5 TeV gamma primary at 107 m core distance.

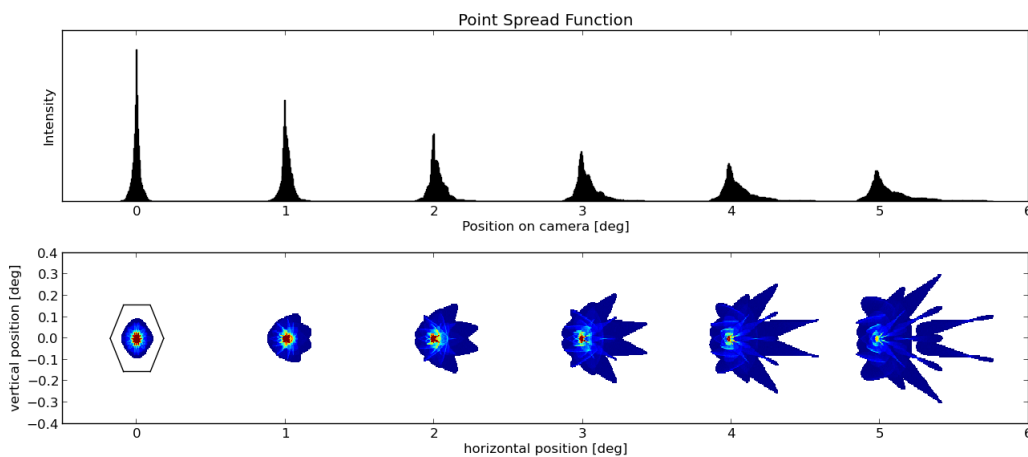


**Figure 3.** IACT Point Spread Function (PSF) for angles of 0-5° from the optical axis. Minimal PSF without mirror misalignment options. The structures are an effect of the outermost mirror segments.

Right now, we have over 80 million events simulated, statistics still rising.

2b. Also, from the same CORSIKA output, the HiSCORE detector response is simulated with sim\_score [7], a custom simulation software based on the IACT package, to determine the core position/resolution and shower direction/angular resolution of the pure array and to evaluate different array layouts and electronic systems.

### 3. Simulation results

#### 3.1. Point spread function (PSF)

One MC simulation study is the Point Spread Function (PSF) of our telescope. A good PSF is essential for good image quality and thus for good reconstruction. The mirror dish of our

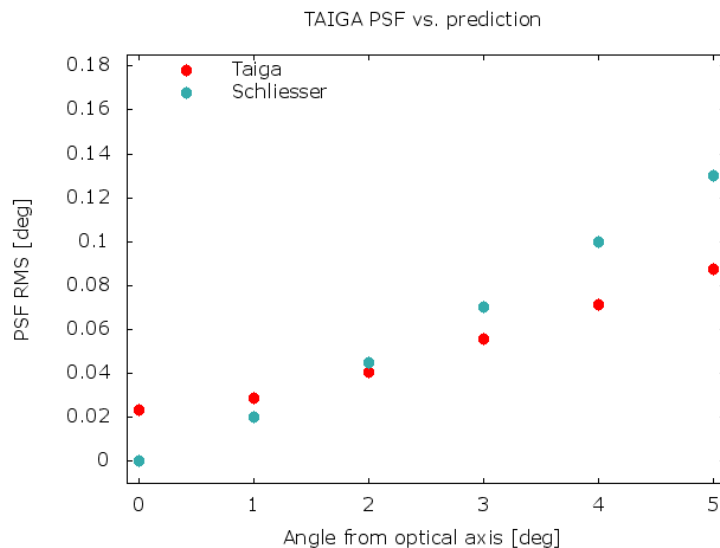


**Figure 4.** Comparison with expected values for the PSF for our  $F/D = 1.1$

telescope is composed of spherical mirror tiles smaller than the overall dish size, as usual for a Davies-Cotton design. This introduces another telescope parameter: The tessellation ratio  $\alpha$ . The tessellation ratio is the relation between individual mirror segment diameter  $d_{tile}$  and the main dish diameter  $D_{dish}$ :

$$\alpha = \frac{d_{tile}}{D_{dish}} \quad (1)$$

Therefore, the bigger the tessellation ratio, the bigger the influence of the individual mirror tiles. With the high field of view (FoV) of about  $8^\circ$  and a tessellation ratio of 0.13, the aberration effects of the mirror structure come into play. Therefore their impact needs to be evaluated.

Compared to the size of a single pixel, the psf shows that even for an angle of  $5^\circ$  to the optical axis, the PSF is still significantly smaller than a pixel (compare Fig. 3). Our PSF is not as good as the predictions made bei Schliesser and Mirzoyan [11] imply (see Fig. 4), but this is expected since our tessellation ratio is larger, increasing the effect of aberrations of the spherical mirror tiles.

### 3.2. Gamma-hadron separation

In a shower sampling array, the steepness of the air shower's light density function is used for primary particle identification [9]. In the low energy range ( $<10$  TeV) however this method works only poorly, especially for gammas and protons [7].

In this range, IACT image analysis is the far more powerful tool to identify the primary's nature.

The parameter that is used for separating the different kinds of primaries with an IACT is the width of the camera image [13], derived from the second moment of the intensity distribution after image cleaning. This width depends mainly on primary energy ( $E$ ), impact parameter ( $d$ ) (e.g. distance between telescope and shower core) and the type of the primary. With the first two parameters measurable by the shower front sampling array, the parameter left is the type, which determines the distribution's shape. Proton showers have a broader width distribution due to their hadronic shower components. To separate gammas from hadrons, a width cut can be applied. The parameter  $Q$  shows the quality of this cut:

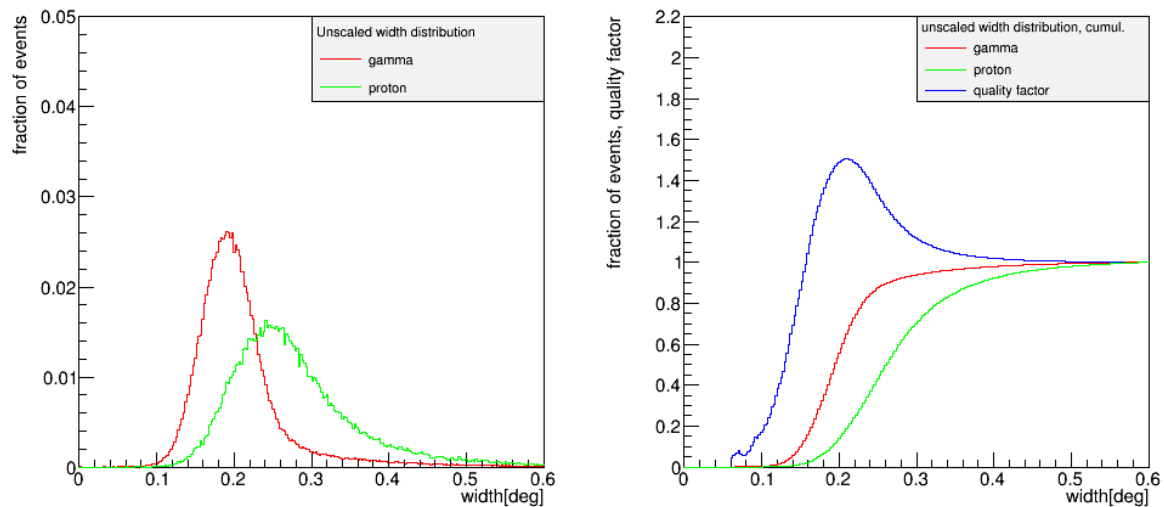


**Figure 5.** Raw width distribution for showers from the zenith in the energy range of 0.5-50 TeV. Red: Gammas, Green: Protons. Left: Differential distribution. It can be seen that the proton distribution is broader than the gamma distribution and a bit shifted towards bigger widths, but the two peaks still overlap much. Right: Cumulative distribution and quality factor  $Q$  for the width cut at. If a cut is made on the raw data, the maximum quality factor is less than 1.5

$$Q = \frac{\epsilon_\gamma}{\sqrt{\epsilon_p}} \quad (2)$$

with

$$\epsilon_i = \frac{n_i(< w)}{n_i} \quad (3)$$

However, the distributions for gammas and protons overlap considerably due to the varying core distances, so that a cut on this parameter is not satisfying (see fig. 5). To improve it, the measured widths are rescaled to the expected value for a gamma-ray induced shower. For this, a three-dimensional lookup-table is generated from MC data, with the parameters core distance, image size and expected width. Then, each event's width is divided by the respective lookup-table entry (speak: scaled), which makes the gamma and the proton distribution peaks move apart (see fig. 6). This is the point where the combination takes place: To find the right lookup-table entry, core distance and zenith angle are reconstructed from the sampling array, and we get the Hybrid Scaled Width (HSCW):

$$HSCW = \frac{w_{tel}}{w_{MC}^\gamma(d_{array}, size_{tel})} \quad (4)$$

Scaling the width increases the quality factor from about 1.4 to almost 2.2, which is significantly better than the quality for pure HiSCORE reconstruction, which achieves only a Q-factor of 1 at the threshold and only approaches 2 at several 100s of TeV. [7]

The results shown in fig. 5 and 6 are the width values. For now, we took the core position for finding the correct lookup-table entry for scaling directly from the MC data. For a first estimate on TAIGA's combined reconstruction quality, we'll randomize the MC core position by

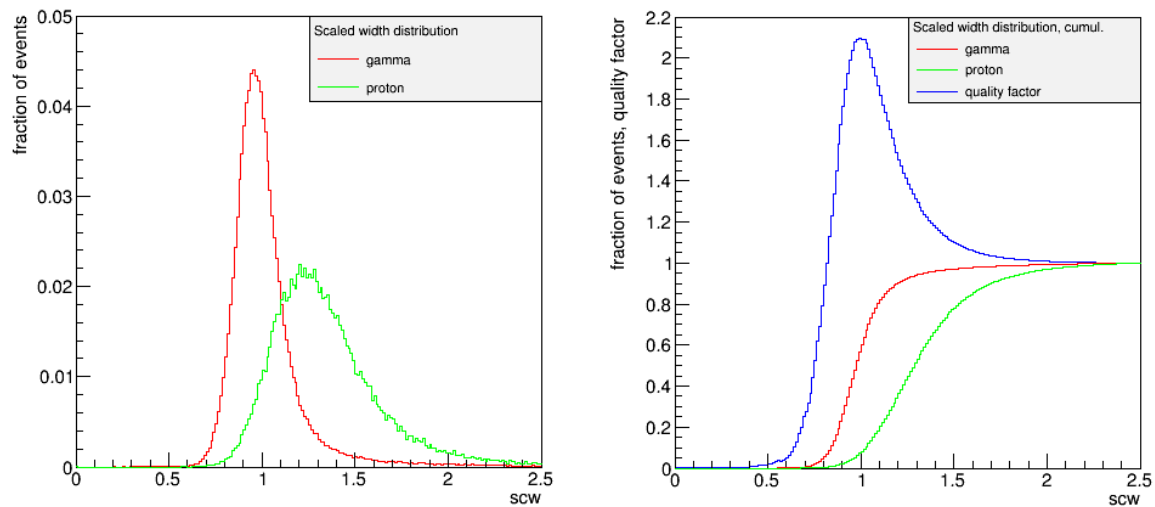


**Figure 6.** Hybrid scaled width (HSCW) distribution for showers from the zenith in the energy range of 0.5-50 TeV. Red: Gammas, Green: Protons. Left: Differential distribution. Compared to figure 5, the gamma and the proton distribution have moved apart significantly. Right: Cumulative distribution and quality factor  $Q$  for the width cut. If a cut is made on the HSCW, the maximum quality factor is almost 2.2

the HiSCORE core resolution and use this randomized core position in the width scaling (toy core simulation). We expect the quality to decrease only little, down to about 2.0.

As a next step, a full hybrid simulation is planned, including a combination of reconstruction algorithms. The monoscopic direction information from the IACT image will be taken into account in the reconstruction of core position from the array, lowering the uncertainties on this parameter, and the gamma-hadron separation by shower front profiling of the array will be combined with the image reconstruction. We expect to improve the  $Q$ -factor at low energies to 3.

Typical stereoscopic systems of Cherenkov telescopes achieve a gamma-hadron separation  $Q$ -factor using the mean scaled width cut of about 6. The often stated factor of  $10^4$  results from combining the width and directional cut (separating the isotropic hadrons by a tight angular cut around the point source of interest). This cut can be done with the hybrid array on a similar quality level, since the angular resolution of the timing array alone is comparable to stereoscopic IACT systems. Here however, we only state the width cut quality.

#### 4. Conclusion and outlook

The TAIGA hybrid system is the first to combine the strengths of Cherenkov timing arrays and IACT telescopes. Our telescope design concept gives a good imaging quality as shown by the PSF. The combination of IACTs with the HiSCORE timing array will result in an improved gamma-hadron separation and a maximisation of the effective area.

The next step is a toy core analysis, then a full hybrid simulation both for array and IACT.

#### Acknowledgements

We acknowledge the support of the Russian Federation Ministry of Education and Science (agreements N 14.B25.31.0010,N2014/51, project 1366, zadanie N 3.889.2014/K ), the Russian

Foundation for Basic research (grants 13-02-00214, 15-02-10005, 13-02-12095), the Helmholtz association (grant HRJRG-303), and the Deutsche Forschungsgemeinschaft (grant TL 51-3)

## References

- [1] Tluczykont M *et al* 2014 The HiSCORE concept for gamma-ray and cosmic-ray astrophysics beyond 10 TeV *Astropart. Phys.* **42**-53
- [2] Hinton J A and Hofmann W 2009 Teraelectronvolt Astronomy *Ann.Rev.Astron.Astrophys.***47** 523-65
- [3] Heck D *et al* 1998 Report *FZKA 6019*, available from [http://www-ik.fzk.de/corsika/physics\\_description/corsika\\_phys.html](http://www-ik.fzk.de/corsika/physics_description/corsika_phys.html)
- [4] Kalmykov N N, Ostapchenko S S, and Pavlov A I 1997 *Nucl. Phys. B (Proc. Suppl.)* **52B** 17
- [5] Fesefeldt H 1985 Report **PITHA-85/02**
- [6] Bernlöhr K 2008 Simulation of imaging atmospheric Cherenkov telescopes with CORSIKA and sim\_telarray *Astropart. Phys.* 149-58
- [7] Hampf D, Tluczykont M and Horns D 2012/13 Event reconstruction techniques for the wide-angle air Cherenkov detector HiSCORE *Nucl. Inst. Meth. in Phys. Res. A* 137-46
- [8] Tluczykont M *et al* 2011 *Adv. Sp. Res.* **48** 1935-41S.
- [9] Budnev N *et al* 2015 The Tunka experiment: from cosmic ray to gamma-ray astronomy *these proceedings*
- [10] Tluczykont M *et al* 2015 Towards gamma-ray astronomy with timing arrays *these proceedings*
- [11] Schliesser A and Mirzoyan R 2005 Wide-field prime-focus imaging atmospheric Cherenkov telescopes: A systematic study *Astrop. Phys.***24** 382-90
- [12] Schröder F G *et al* 2012 *AIP Conf. Proc* **1535** 111
- [13] Hillas A M 1985 Cerenkov light images of EAS produced by primary gamma *Int. Cosm. R. Conf.* **3** 4458.